

## DEEP LEARNING APPROACH TO INLINE QUALITY RATING AND MAPPING OF MULTI-CRYSTALLINE SI-WAFERS

Matthias Demant<sup>1,3</sup>, Patrick Virtue<sup>2,3</sup>, Aditya S. Kovvali<sup>1</sup>, Stella X. Yu<sup>2,3</sup>, Stefan Rein<sup>1</sup>

<sup>1</sup>Fraunhofer ISE, Heidenhofstraße 2, D-79110 Freiburg, Germany

<sup>2</sup>University of California, Berkeley, CA 94720, USA

<sup>3</sup>International Computer Science Institute, 1947 Centre Street, Berkeley, CA 94704, USA

### ABSTRACT:

This work shows the first successful application of convolutional neural networks (CNN) for material characterization and process control in solar cell production. We present a fully data-driven machine learning approach for inline quality rating and quality mapping of as-cut multi-crystalline Silicon (mc-Si) wafers. We use Photoluminescence (PL) images to image crystallization related defects in the wafers. We show that we can learn how to quantify these defect patterns based on empirical data and derive a meaningful wafer representation directly from the high-resolution input images by means of deep CNNs. This end-to-end regression model predicts solar cell efficiencies with mean errors of 0.12% for materials of bricks not presented in the training set, which is 25%<sub>rel</sub> better than our classical methods based on feature engineering. Moreover, we visualize the expected quality distribution for each sample within a spatially resolved activation map. The mapping procedure gives an insight into the “black box” neural network and shows that the quality distribution is in accordance to the expectations of domain experts and similar to spatially resolved quality data like the image of the dark saturation current density ( $j_0$ ). More details on learning and mapping will be reported within two studies elsewhere.

Keywords: Multi-Crystalline Silicon, Convolutional Neural Networks, CNN, Regression Activation Mapping, Material Rating, Semantic Representation, PERC

### 1 INTRODUCTION

The rating of mc-Si wafers with regard to the expected solar cell quality directly after wafering allows a fast and cost efficient material control for crystal growers and solar cell manufacturers.

This paper presents results from two comprehensive studies on learning quality rating [1] and quality mapping [2] of as-cut multi-crystalline Si-wafers via convolutional neural networks (CNN) for regression.

We use Photoluminescence (PL) images [3] as input for a convolutional neural network to predict the current-voltage (IV) parameters of the solar cells. PL-images are suitable for an inline analysis of as-cut samples since they reveal crystallization-related defects in mc-Si materials, which correlate with solar cell quality [4].

Nevertheless, for as-cut wafers a determination of the bulk lifetime of excess charge carriers is limited due to the high surface recombination. This impacts the rating of high quality material for high quality solar cell processes. This study investigates high performance materials [5]

and passivated emitter and rear cells (PERC) [6] to address this matter.

In previous works [7-13], feature engineering methods have been applied to extract features according to domain knowledge. The design of domain-relevant features is challenging as PL-intensities and PL-contrasts vary in the continuous image space. The defect patterns superimpose in the images and interact during the process [14-16] for example within high-temperature or surface structuring processes.

A meaningful representation of the PL-images with regard to solar cell quality can be learned within deep convolutional neural networks (Section 2). The training of the model requires a representative data set which is acquired within a huge experiment (Section 3). The proof of generalizability for complex models needs to be evaluated on “unknown” test data not presented in training data (Section 4). For a deeper understanding and acceptance of our approach in the PV community we visualize what has been learned in the PL-image (Section 5).

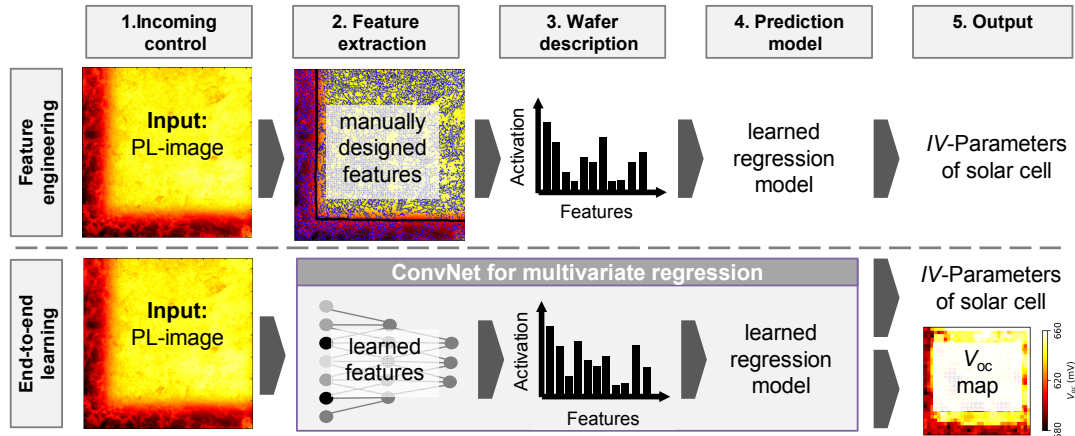


**Figure 1:** (Top row) Overview of the pattern recognition pipeline for material rating based on as-cut mc-Si wafers. In the middle row the classical approach uses features engineered by human experts and in the bottom row the end-to-end rating learns feature extraction and prediction in the same convolutional neural network. In addition to quality prediction, the regression activation map (RAM) reveals the spatial distribution of open-circuit voltage ( $V_{oc}$  map) learned by the network

## 2 APPROACH

### 2.1 Pattern recognition pipeline

An overview of the pattern recognition pipeline for material rating based on as-cut mc-Si wafers is shown in Figure 1. Wafers from different materials are measured in an incoming control and PL-images are analyzed. The PL-features are extracted and combined in a histogram which forms the basis of a rating model to predict the IV-parameters of the solar cells.

Following to the classical feature engineering approach [17], the extraction of features is based on a combination of human defined filters. The optimization of the regression model for  $V_{oc}$  prediction is based on empirical data.

Within the end-to-end rating model the feature representation and the regression parameters are learned within the same optimization step and are not based on a manually designed feature definition.

### 2.1 Regression network and activation map

Recently, innovations in deep learning have led to significant breakthroughs in computer vision tasks from classification [18] to localization of objects and activities within an image [19]. Convolutional neural networks with dense connections have been particularly effective in these tasks, primarily due to its additional connections between layers that improve accuracy by allowing data to propagate more efficiently through the very deep network. We convert densely connected network architecture from an object recognition network to a multivariate regression network that predicts solar cell efficiency, open-circuit voltage, short-circuit current and fill factor within one model.

We want to analyze, what has been learned in the model. An activation map [19] with spatial coordinates can be computed for a given PL-image as input to reveal the learned quality distribution of our regression model. It can show us how the network rates dislocations and regions of reduced lifetime due to contaminations from the crystallization crucible. The map is qualitatively compared to  $j_0$ -images of the solar cell [20] to confirm the meaningful interpretation of the patterns.

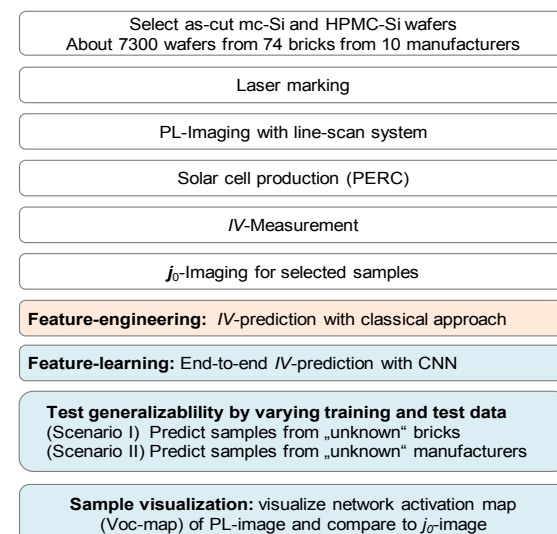


**Figure 2:** Schemata of the experiment

## 3 EXPERIMENTAL

As deep neural networks require large training datasets for successful optimization, we collect a wide variety of experimental data.

Figure 2 gives an overview of the experimental approach for the collection and evaluation of this data. The comprehensive data set allows a proof of generalizability by testing the model with completely unknown data.

The experimental process steps are as following: the wafers are sampled from different positions of various bricks from ten manufacturers. The data set contains mc-Si and HPMC-Si material. The samples are laser-marked and PL-images are measured within an incoming-control with a line-scan PL-system [21]. The wafers are processed to PERC solar cells within an industrial production line. IV-parameter and  $j_0$ -images [20] are measured after solar cell production.

We evaluate the measured images based on the feature-engineering approach [12] and the proposed feature-learning approach. The models are trained with approximately 3000 wafers and tested with the remaining samples. This work presents the results of Scenario I where no wafers of the same brick are in test and training set. In Scenario II all wafers of the tested manufacturer are removed from the training set, which will be presented in [1].

The presented regression activation maps (RAM) are based on a network trained for  $V_{oc}$  prediction with PL-images as input. For the computation of the RAM the PL-image is passed through the network. No additional information about  $V_{oc}$  from current-voltage measurement is required. The RAM is compared to the  $j_0$ -images to visualize what has been learned in the network.

## 4 RESULTS ON CELL QUALITY PREDICTION

The presented prediction model is capable to quantify complex defect structures and predict the solar cell efficiency (Figure 3) and open-circuit voltage (Figure 4) with low mean absolute error for the prediction of unknown bricks (Table I). The prediction of short-circuit current density ( $J_{sc}$ ) and fill factor are less accurate. The network improves the rating with manually designed features by about 25%rel for efficiency prediction.

**Table I:** Prediction of unknown bricks

Method		Eta [%]	$V_{oc}$ [mV]	$J_{sc}$ [mA/cm <sup>2</sup> ]	FF [%]
Designed features	MAE	0.16	2.73	0.17	0.32
	Corr	0.88	0.89	0.83	0.53
Learned features	MAE	0.12	2.15	0.15	0.28
	Corr	0.93	0.93	0.87	0.67

MAE = Mean absolute error in unit of parameter

Corr = Pearson correlation coefficient in [-1, 1]

The network converges rapidly during training and overcomes the bias-variance trade-off during testing: on the one hand, the network is capable to quantify defect patterns within a complex network structure and on the other hand, the model is generalizable to predict unknown data. The prediction can be computed within only a few milliseconds.

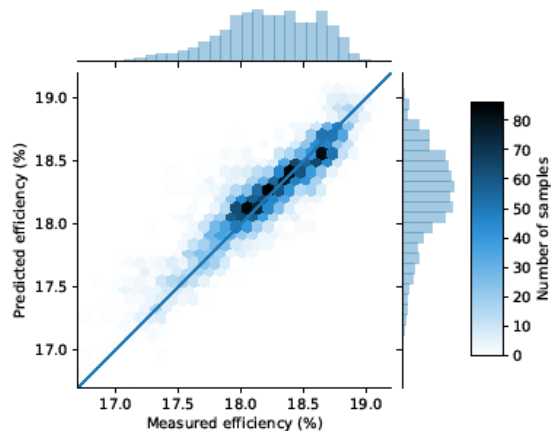


**Figure 3:** Result on efficiency prediction

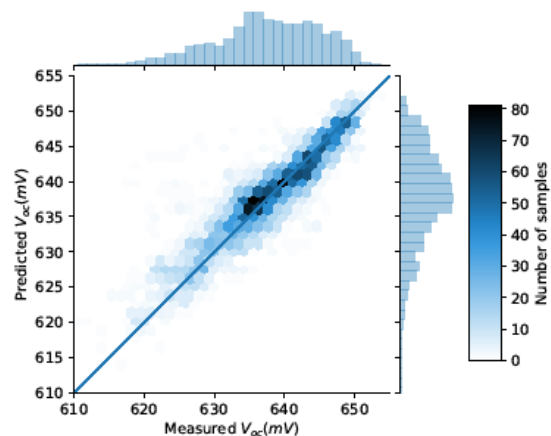


**Figure 4:** Result on open-circuit voltage prediction

Details on model and rating, as well as the prediction results for materials from unknown manufacturers will be available in the report on our full study [1].

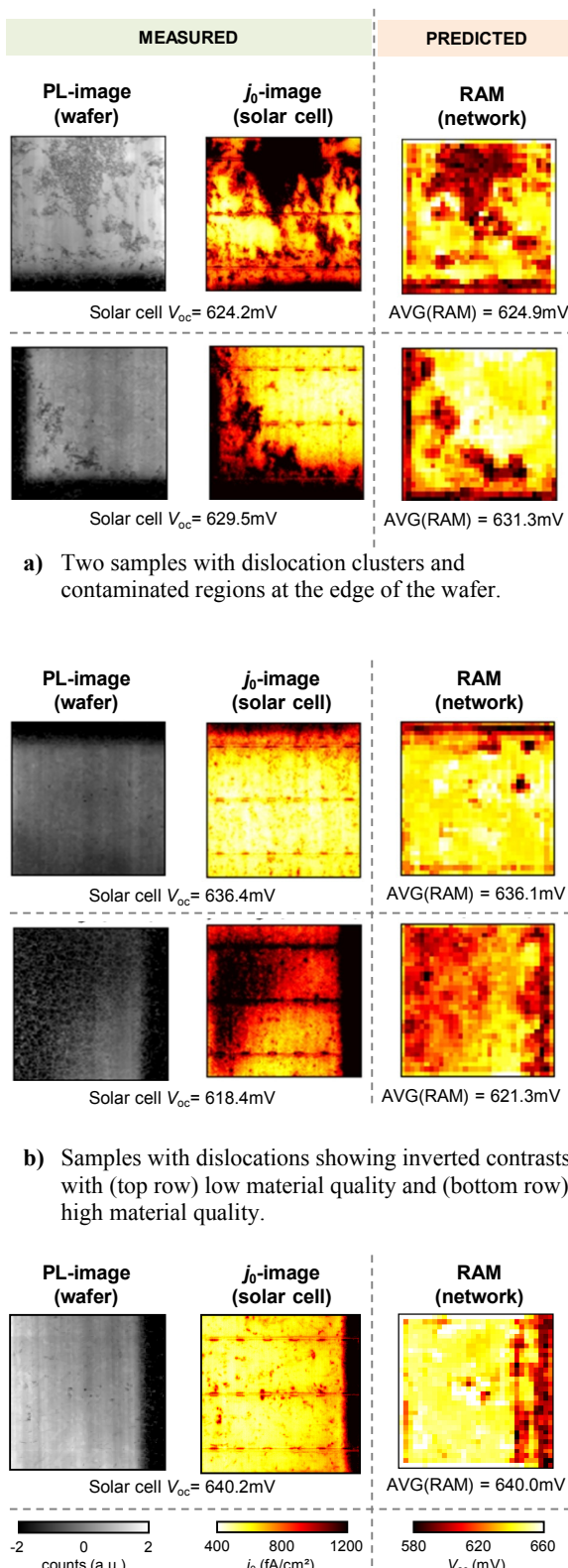
## 5 RESULTS ON VISUALIZING WHAT HAS BEEN LEARNED IN THE NETWORK

The network learns a prediction model based on the PL-image as input and the solar cell parameter as output, here the open-circuit voltage. What has been learned in the network? The activation map (AM) is a technique, which reveals how different image regions are rated in the network purely based on the PL-image and the trained model. Note that no human input has been given to the network, except the PL-input image and the  $V_{oc}$  during model training.

The average of the activation map for regression (RAM) is the prediction result. Thus, the map can be scaled to Volts.

The comparison of PL-inputs, the RAM of the network and the measured  $j_0$ -images in Figure 5a) show strong similarities between predicted and measured quality. The network assigns low quality values to dislocation clusters and contaminated regions.

Even for samples with inverted contrast in Figure 5b) the network distinguishes the effect of different structures which are comparable to the  $j_0$ -images. The distributed  $V_{oc}$  values result in quality estimation with small error.



**c)** Failure case shows activations, which are not directly connected to crystallization defects.

**Figure 5:** Triplets of (left) PL-image of as-cut wafer, (center) the  $j_0$ -image measured after solar cell production and (right) the regression activation map learned by the network for  $V_{oc}$ -prediction. The measured and predicted  $V_{oc}$  values are annotated below each sample.

Only few examples show artefacts not being related to crystallization defects. For example the line like structure in the RAM in Figure 5c) might be connected to a strong saw-mark.

Further errors might be connected to the low resolution of the RAM with 32px × 32px. Also the exact defect position in the RAM may vary due to the large receptive field of each neuron in PL-image space.

## 6 CONCLUSION

This work showed the first successful application of CNNs for material characterization and process control in solar cell production. We identified a promising neural network architecture, which requires an intensive training procedure but allows for a generalizable and inline applicable prediction of the material quality. Further details on the learning algorithm will be available in our report in [1].

We applied an activation mapping technique to reveal what has been learned by the network. The regression activation map is in accordance with the expectations of a human expert: regions with reduced lifetime and structural defects in the PL-images are rated as regions with reduced quality in the RAM. A comparison of the network activation map shows the high similarity of the predicted quality distribution in wafer coordinates to the measured  $j_0$ -images. A detailed introduction to this mapping technique and further visualization results will be given in [2].

The model can be extended easily by adding e.g. spatially resolved grain boundary data [22] or a brick lifetime parameter [23] to the prediction model, which can offer additional information for material characterization.

## ACKNOWLEDGEMENTS

This work was supported by German Federal Ministry of Economic Affairs and Energy (BMWi) in the project "Q-Crystal" under the contract number 0324103A.

M. Demant was supported by a scholarship of the German Academic Exchange Service (DAAD) within the program FITweltweit.

## REFERENCES

- [1] M. Demant, *et al.*, "Learning quality rating of multicrystalline Si-wafers via convolutional regression networks," submitted 2018.
- [2] M. Demant, *et al.*, "Visualizing material quality and similarity of mc-Si wafers learned by convolutional regression networks," submitted 2018.
- [3] T. Trupke and R. A. Bardos, "Photoluminescence: a surprisingly sensitive lifetime technique," in *Proceedings of the 31st IEEE Photovoltaic Specialists Conference*, Orlando, Florida, USA, 2005, pp. 903-906.
- [4] J. Haunschild, *et al.*, "Quality control using luminescence imaging in production of mc- solar cells from UMG feedstock," in *Proceedings of the 35th IEEE PVSC*, Honolulu, Hawaii, USA, 2010, p. in print.
- [5] C. W. Lan, *et al.*, "Grain control in directional solidification of photovoltaic silicon," *Journal of Crystal Growth*, vol. 360, pp. 68-75, 2012.
- [6] M. A. Green, "The Passivated Emitter and Rear Cell (PERC): From conception to mass production," *Solar Energy Materials and Solar Cells*, vol. 143, pp. 190-197, 2015.
- [7] M. Demant, *et al.*, "Analysis of luminescence images applying pattern recognition techniques," in *Proceedings of the 25th EU-PVSEC*, Valencia, Spain, 2010, pp. 1078-1082.
- [8] W. McMillan, *et al.*, "In-line monitoring of electrical wafer quality using photoluminescence imaging," in *Proceedings of the 25th European Photovoltaic Solar Energy Conference and Exhibition*, Valencia, Spain, 2010, pp. 1346-51.
- [9] B. Birkmann, *et al.*, "Analysis of Multicrystalline Wafers Originating from Corner and Edge Bricks and Forecast of Cell Properties," in *26th European Photovoltaic Solar Energy Conference and Exhibition*, Hamburg, 2011, pp. 937 - 940.
- [10] B. True, *et al.*, "Image processing techniques for correlation of photoluminescence images of as-cut wafers with final cell IV parameters," in *Proceeding of the 26th EU-PVSEC*, Hamburg, Germany, 2011, pp. 1-4.
- [11] M. Demant, *et al.*, "Modelling of physically relevant features in photoluminescence images," *Energy Procedia*, vol. 27, pp. 247-52, 3-5 Apr 2012.
- [12] M. Demant, *et al.*, "Inline quality rating of multicrystalline wafers based on photoluminescence images," *Progress in Photovoltaics: Research and Applications*, pp. 1533-46, 2015.
- [13] T. Trupke and R. A. Bardos, "Wafer imaging and processing method and apparatus," ed: Google Patents, 2017.
- [14] S. McHugo, *et al.*, "Gettering of metallic impurities in photovoltaic silicon," *Applied Physics A*, vol. 64, pp. 127-137, 1997.
- [15] A. Bentzen and A. Holt, "Overview of phosphorus diffusion and gettering in multicrystalline silicon," *Materials Science and Engineering B*, vol. 159-60, pp. 228-34, 2008.
- [16] S. Castellanos, *et al.*, "High-performance and traditional multicrystalline silicon: Comparing gettering responses and lifetime-limiting defects," *IEEE Journal of Photovoltaics*, vol. 6, pp. 632-640, 2016.
- [17] M. Demant, *et al.*, "Inline quality rating of multicrystalline wafers based on photoluminescence images," *Progress in Photovoltaics: Research and Applications*, 2015.
- [18] A. Krizhevsky, *et al.*, "Imagenet classification with deep convolutional neural networks," in *Advances in Neural Information Processing Systems*, 2012, pp. 1097-1105.
- [19] B. Zhou, *et al.*, "Learning deep features for discriminative localization," in *Computer Vision and Pattern Recognition (CVPR), 2016 IEEE Conference on*, 2016, pp. 2921-2929.
- [20] M. Glatthaar, *et al.*, "Evaluating luminescence based voltage images of silicon solar cells," *Journal of Applied Physics*, vol. 108, pp. 014501/1-5, 2010.
- [21] H. Höffler, *et al.*, "Comparison of line-wise pl-imaging and area-wise pl-imaging," *Energy Procedia*, vol. 124, pp. 66-75, 2017/09/01 / 2017.

- [22] A. S. Kovvali, *et al.*, "About the Relevance of Defect Features in As-Cut Multicrystalline Silicon Wafers on Solar Cell Performance," in *Silicon PV*, Lausanne, Switzerland, 2018.
- [23] B. Mitchell, *et al.*, "PERC solar cell performance predictions from multicrystalline silicon ingot metrology data," *IEEE Journal of Photovoltaics*, vol. 7, pp. 1619-1626, 2017.